New parametrization of the optical potential

C. Hartnack[1,2] and J. Aichelin[1]
[1] *Laboratoire de Physique Nucléaire, Université de Nantes, F-44072 Nantes Cedex 03, France*
[2] *Gesellschaft für Schwerionenforschung, D-64220 Darmstadt, Federal Republic of Germany*
(Received 5 October 1993)

Recent experimental results have shown that the optical potential is much more repulsive at energies above 400 MeV/nucleon than believed at the beginning of the eighties. Taking these new data into account we present a new parametrization of the optical potential, of the underlying bare nucleon-nucleon interaction, as well as of its expectation value for Gaussian wave functions as used in quantum molecular dynamics calculation. For the case Au + Au $b = 3$ fm we compare the result for several observables with that obtained employing the old parametrization.

PACS number(s): 24.10.Ht, 13.75.Cs, 21.65.+f

The influence of the optical potential on observables measured in heavy ion reactions has been widely investigated in recent years employing microscopic models like the Boltzmann-Uehling-Uhlenbeck model or the quantum molecular dynamics approach [1,2]. It has been shown that this influence is far from negligible. Comparing the results obtained for different static equations of state (EOS) one finds differences of the same order of magnitude such as comparing a static with a momentum dependent EOS, yielding the same ground-state properties. Therefore a precise modeling of the optical potential is necessary before one can draw any firm conclusion.

In 1987, when one started to investigate the influence of the optical potential on different observables [1] we took advantage of an analysis of p-Ca data of Arnold *et al.* [3] in the framework of a relativistic Dirac equation. The Schrödinger equivalent potential extracted from this analysis is displayed in Fig. 1 as full circles. Assuming that the optical potential $U(p)$ is connected with the bare interaction by

$$U(p) = \int_{p'<k_F} d^3p' V(p-p') / \int_{p'<k_F} d^3p', \tag{1}$$

the available data points of Arnold *et al.* [3] and Passatore [4] are allowed to fit the bare interaction. We obtained

$$V(p-p') = -54 + 1.58\{\ln[(p-p')^2 a + 1]\}^2 \text{ (MeV)} \tag{2}$$

with $a = 5 \times 10^{-4}\, c^2/\text{MeV}^2$. The optical potential and the bare interaction are given by the dashed dotted and the dotted lines, respectively, in Fig. 1.

New parametrization of the optical potential. Recently this old analysis of Arnold *et al.* has been superseded by a much more extensive analysis of a wealth of data by Hama *et al.* [5]. The theoretical framework there is the same but the extracted Schrödinger equivalent potential has now a quite different form. The new data points are displayed as open circles in Fig. 1. They have been obtained by using the program GLOBAL.FOR provided by the authors of Ref. [5]. Assuming a bare interaction of $[\Delta p = (p-p')^2]$

$$\begin{aligned} V(p-p') = &-0.0257(\Delta p)^{3/4} + 0.1275(\Delta p)^{+1/4} \\ &-0.08058(\Delta p)^{-1/4} + 0.0058(\Delta p)^{-3/4} \\ &-0.00006(\Delta p)^{-5/4}, \end{aligned} \tag{3}$$

we calculate the optical potential with help of Eq. (1). The result is shown as the dashed line in Fig. 1, the bare interaction [Eq. (3)] as a full line.

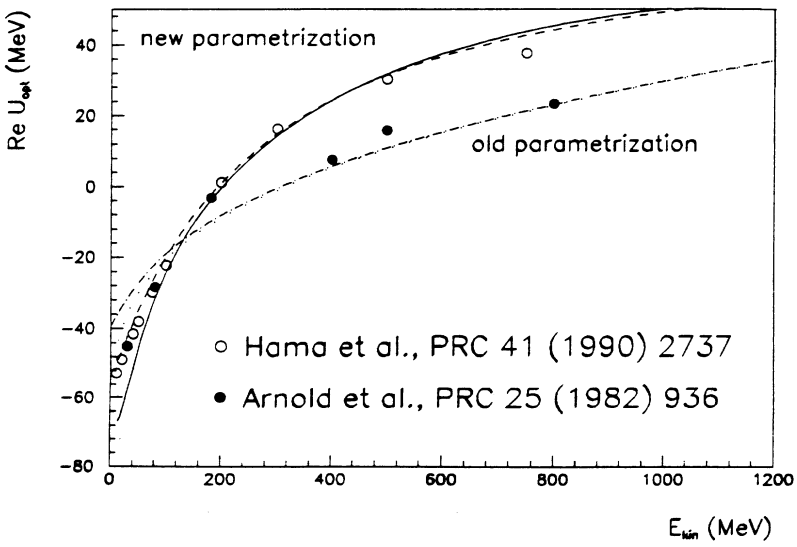

FIG. 1. The new and the old parametrization of the optical potential as well as of the bare interaction as compared to the data points of Arnold *et al.* and Hama *et al.*

In the quantum molecular dynamics (QMD) [1,2] approach the nucleons are represented by Gaussian wave functions

$$\phi_\alpha(x_1,t)=\left(\frac{2L}{\pi}\right)^{3/4} e^{-[x_1-x_\alpha(t)]^2 L} e^{ix_1 p_\alpha(t)} e^{-ip_\alpha^2(t)t/2m}. \tag{4}$$

The parameters x_α, p_α are time dependent; L is fixed and equal to $1/2.16$ fm^2. The time evolution equations [6] are obtained by a variational principle which yields

$$\dot{\bar{x}}_\alpha=\frac{p_\alpha}{m}+\nabla_{p_\alpha}\sum_\beta\langle U_{\alpha\beta}\rangle, \tag{5}$$

$$\dot{p}_\alpha=-\nabla_{\bar{x}_\alpha}\sum_\beta\langle U_{\alpha\beta}\rangle \tag{6}$$

with $\bar{x}_\alpha=x_\alpha=x_\alpha+(p_\alpha/m)t$. The potential U is obtained by folding of the bare interaction $V(p-p')$ [Eq. (3)] with the wave functions [Eq. (4)]. This calculation has to be performed numerically. The result is given in Fig. 2. It can be easily fitted by a function of the form

$$\langle U_{\alpha\beta}(p_\alpha-p_\beta)\rangle=0.0667-\frac{0.0589}{(\mathbf{p}_\alpha-\mathbf{p}_\beta)^2+0.4837}, \tag{7}$$

where all quantities are given in powers of GeV, respectively GeV/c.

Equation of state. One of the major motivations for studying heavy ion collisions at intermediate energies is the determination of the nuclear equation of state.

$$E/N\left(\frac{\rho}{\rho_0},T\right)=\left\langle E_{\rm kin}\left(\frac{\rho}{\rho_0},T\right)\right\rangle +W_{\rm static}\left(\frac{\rho}{\rho_0}\right)\left[+W_{\rm opt}\left(\frac{\rho}{\rho_0},T\right)\right]. \tag{8}$$

At zero temperature T and for a ground state density ρ_0 of 0.17 nucleon/fm^3, $\langle E_{\rm kin}\rangle$ is given by $22.95(\rho/\rho_0)^{2/3}$ (MeV/nucleon). We will assume that $W_{\rm opt}$ is a two-body interaction and hence in nuclear matter $\sim\rho/\rho_0$.

The contribution of the optical potential to the nuclear EOS at zero temperature is given by

$$W_{\rm opt}\left(\frac{\rho}{\rho_0},T=0\right)=\frac{1}{2}\frac{\int_{p',p<k_F}d^3p'd^3pV(p-p')}{\int_{p'<k_F}d^3p'\int_{p'<k_F}d^3p}\frac{\rho}{\rho_0}, \tag{9}$$

where we integrate over the momentum up to the Fermi momentum $k_F=(3\pi^2\rho/2)^{1/3}$. The factor of 1/2 is present because $W_{\rm opt}$ is the potential energy and not the potential.

For the static potential energies one chooses a parametrization of the form

$$W_{\rm static}\left(\frac{\rho}{\rho_0}\right)=\frac{\alpha}{2}\frac{\rho}{\rho_0}+\frac{\beta}{\gamma+1}\left(\frac{\rho}{\rho_0}\right)^\gamma \tag{10}$$

Two of the three parameters are determined by the binding energy of -16 MeV at normal nuclear matter density ρ_0. The third parameter can be expressed in terms of the compressibility. In the past essentially two parametriza-

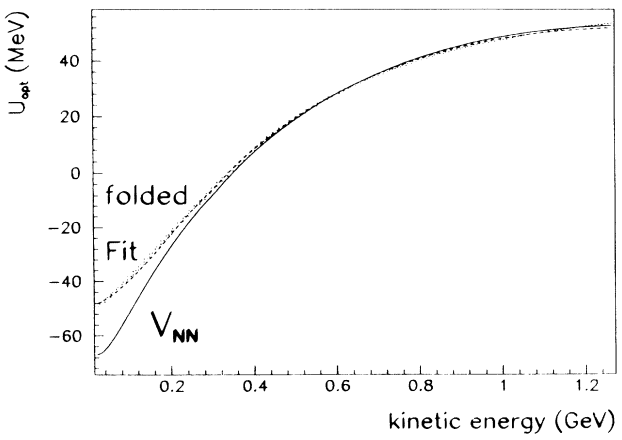

FIG. 2. The bare interaction, the bare interaction folded with Gaussian wave functions as employed in QMD calculations, and a fit by this function as a function of the energy.

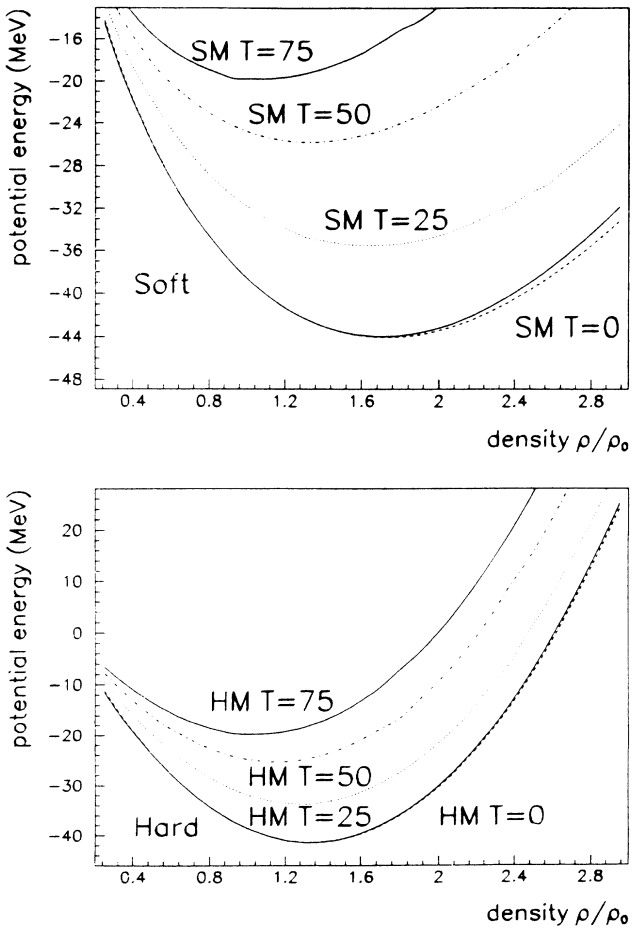

FIG. 3. The potential energy per nucleon $W_{\rm opt}(\rho/\rho_0,T)$ as a function of the density for different temperatures. On the top we see $W_{\rm opt}$ for the soft equation of state, at the bottom for the hard equation of state.

TABLE I. Parameters for the different equations of state.

EOS	Opt. potential	Compressibility (MeV)	α (MeV)	β (MeV)	γ
S	no	200	−382.52	328.27	1.155
SM	yes	200	−3189	3176	1.011
H	no	380	−125.16	70.91	2.0
HM	yes	380	−63.13	49.42	2.12

tions, dubbed soft and hard EOS, which mark the boundaries of the expected range of compressibilities, have been employed. The potential which enters the time evolution equations can be obtained by

$$U = (1/\rho)[d(W\rho)/d\rho]. \tag{11}$$

It has been proven that for exploring the EOS it is desirable to compare static potential energies W_{static} (despite being unrealistic) with momentum dependent potentials $W_{\text{static}} + W_{\text{opt}}$ which on the one hand reproduce the measured optical potential and on the other hand give in cold nuclear matter the same EOS as the static EOS. If we would like to have the same compressibility as the corresponding static EOS, we have to readjust α, β, and γ. The values for the standard hard and soft EOS as well as for those with momentum dependent interactions are displayed in Table I.

For SM we observe an exponent γ very close to 1. This means that the static part of the potential is almost linear in the density and therefore does not have a pronounced minimum. Furthermore it varies very little with density as compared to all the other equations of state. Therefore, at finite temperature, where the optical potential changes little with density, it cost little energy to yield a high density in the overlap region. Hence we observe high densities ($\approx 3\rho/\rho_0$) already at low beam energies. Whether this is realistic or not is hard to judge. As indicated, from the measured optical potential a momentum dependent nucleon nucleon interaction cannot be extracted in a unique way. Therefore there may be another parametrization which yields the same optical potential which causes less of compression.

As can be seen from Fig. 3, where we present the potential energy/nucleon for the different equations of state, for zero temperature H and HM as well as S and SM agree almost completely for all densities.

In heavy ion reactions the directed beam momentum is quite quickly converted into thermal motion. Therefore, when being compressed, in heavy ion reactions the system is not at zero temperature but, depending on the beam energy, at temperatures between 10 and 100 MeV. A nonzero temperature changes the potential energy/nucleon of the optical potential because we have to replace Eq. (9) by

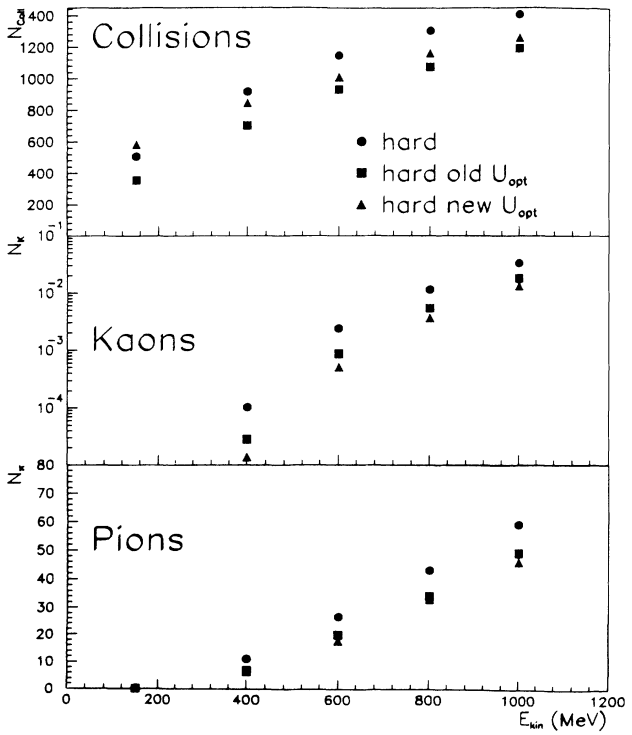

FIG. 4. The number of collisions, and the number of kaons and pions as a function of the energy for the different equations of state.

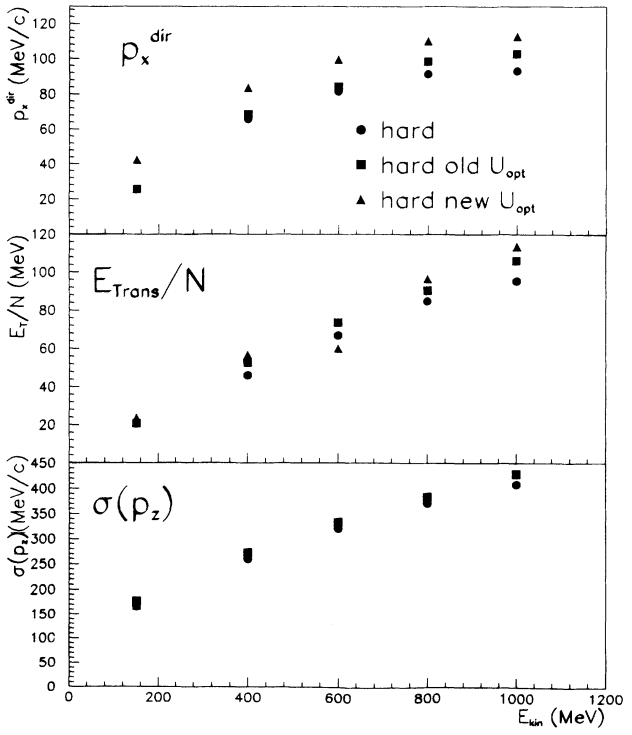

FIG. 5. The flow, the average transverse energy, and width in longitudinal momentum space as a function of the energy for the different equations of state.

$$W_{\rm opt}(\rho/\rho_0, T)$$

$$= \frac{1}{2} \frac{\int g(p,T,\mu) g(p',T,\mu) d^3p' d^3p V(p-p')}{\int g(p',T,\mu) d^3p' \int g(p,T,\mu) d^3p} \frac{\rho}{\rho_0} \qquad (12)$$

where $g(p',T,\mu)$ is the Fermi distribution. T and μ can be calculated numerically if the density and the energy are known.

Figure 3 presents $W_{\rm opt}(T)$ for different temperatures. At the top we see the soft EOS at the bottom the hard EOS. For both equations of state we observe a moderate increase of $W_{\rm opt}(T)$ as compared to the increase of $\langle E_{\rm kin}(T) \rangle$. Therefore we plot the potential energy only. At $T = 75$ MeV an increase of about 25 MeV/nucleon is observed which has to be compared with an increase of about 90 MeV/nucleon of the kinetic energy. The minimum of the potential energy shifts to lower values of the density. We expect therefore the density to become smaller as compared to the hard EOS.

To study the influence of the new parametrization on observables we performed calculations for Au + Au, $b = 3$ fm in the energy range between 150 and 1000 MeV/nucleon.

In Fig. 4 we see from top to bottom the number of baryon collisions and the number of produced kaons and pions. For all energies above 150 MeV/nucleon with a hard EOS the nucleons suffer more collisions than with a momentum dependent interaction. At 150 MeV/nucleon there is the effect that the optical potential is slightly repulsive due to the folding with the Gaussians. The difference between potential energy per nucleon at ρ_0 and $2\rho_0$, which is a measure for the force acting at the interface between projectile and target, is therefore larger for the hard EOS than for HM. Thus we reach a higher compression with HM as compared to H. This effect is not anymore present if the optical potential becomes negative. Therefore for the higher energies the density obtained with H is always larger than that obtained with both HM, and as a direct consequence we see for H a larger number of collisions.

Since the new optical potential is more repulsive at the energies where kaons can be produced ($E_{\rm kin} > 800$ MeV), we expect a further reduction of the kaon yield as compared to the old parametrization. If more energy is stored in the interaction, two baryons have a lower probability to have a sufficient $\sqrt{s}$ to overcome the threshold. At 1 GeV this reduction is about 37%. The pions, on the other hand, are rather insensitive and agree between the statistical errors for both momentum dependent potentials. They are produced in the late stage of the interaction where the system has a high degree of thermalization and therefore the average kinetic energy is between 25 and 100 MeV, depending on the beam energy. At that low energy, the difference between the two optical potentials is not very important.

In Fig. 5 we present from top to bottom the flow measured by $p_x^{\rm dir} = \sum_{i=1}^{N} {\rm sgn}(y_i^{\rm c.m.}) p_x(i)$, the transverse energy $E_T/N = \sqrt{m^2 + p_T^2} - m$ and $\sigma(p_z) = \sqrt{\langle p_z^2 \rangle - \langle p_z \rangle^2}$. At 150 MeV, $p_x^{\rm dir}$ has increased by almost a factor of 2 for HM as compared to H. This is a consequence of the higher density observed as well as of the additional flow generated by a momentum dependent interaction, which is explained in Ref. [1]. In the overlap region of two colliding nuclei we have relative momenta of the size of the beam momentum. Around the overlap region the momenta are around the Fermi momenta. If an optical potential is at work, there is hence a strong potential gradient between both regions, which points—due to geometry—in the transverse direction. The flow, generated by this gradient, is created very early during the reaction where the relative momenta are largest. As a consequence the system is diverted sidewards, and the effective mean free path increases and the density decreases. Therefore, the flow obtained in calculations with optical models is only partly due to the density gradient (as for the static EOS's) and the flow caused by the density gradient is always smaller since the density is less. Despite having almost the same value, the origin of the flow for H and the old optical model is therefore different. Since with the new parametrization the density becomes slightly higher, we obtain additional flow from the now larger density gradient which causes an increase for HM as compared to the others.

The optical potential increases the transverse energy per nucleons slightly but the fluctuations are large there. The stopping measured by $\sigma(p_z)$ is almost identical.

We have presented a parametrization of the optical potential. We observe that most of the observables change only slightly. However, the two that are of importance for the present experiments at GSI, the flow values at low energies [9] as well as the kaon production at high energies [10,11], show the largest changes. For the kaon production, where optical model calculations have underestimated the observed kaon yield by a factor of 3, we observe a further reduction of about 40%. The calculated flow at 150 and 400 MeV/nucleon, however, comes now almost on top of the experimental values.

[1] J. Aichelin *et al.*, Phys. Rev. Lett. **58**, 1926 (1987).
[2] J. Aichelin, Phys. Rep. **202**, 233 (1991).
[3] L. G. Arnold *et al.*, Phys. Rev. C **25**, 936 (1982).
[4] G. Passatore, Nucl. Phys. **A95**, 694 (1967).
[5] S. Hama *et al.*, Phys. Rev. C **41**, 2737 (1990).
[6] J. Aichelin, Prog. Part. Nucl. Phys. **30**, 191 (1993).
[7] H. Stöcker and W. Greiner, Phys. Rep. **137**, 277 (1986).
[8] W. Cassing *et al.*, Phys. Rep. **188**, 361 (1990).
[9] Th. Wienold, GSI Report 93-28.
[10] E. Grosse, Prog. Nucl. Part. Phys. **30**, 89 (1993).
[11] W. Ahner, GSI Report 93-29.